

## CFD modeling: a powerful tool for high efficiency burner design

A. Saponaro<sup>a</sup>, O. Senneca<sup>c</sup>, F. Cerciello<sup>c</sup>, D.J. Brand<sup>d</sup>, M. Torresi<sup>e</sup>, F. Cesareo<sup>e</sup>, M. Valenzano<sup>e</sup>, S. Siena<sup>e</sup>, G. Rago<sup>a</sup>, G. Rossiello<sup>b</sup>, G. Volpi<sup>f</sup>, M. Penati<sup>f</sup>, R. Dadduzio<sup>f</sup>, T. Gianì<sup>f</sup>, M. Rogora<sup>f</sup>, L. Fortunato<sup>a</sup>, V. Panebianco<sup>f,\*</sup>  
vincenzo.panebianco@acboilers.com

<sup>a</sup> Centro Combustione Ambiente S.p.A, Via Milano km 1600, 70023 Gioia del Colle (BA), ITALY

<sup>b</sup> ITEA S.p.A, Via Milano km 1600, 70023 Gioia del Colle (BA), ITALY

<sup>c</sup> Istituto di Ricerche sulla Combustione (IRC), Piazzale Vincenzo Tecchio 80, 80125 Napoli (NA), ITALY

<sup>d</sup> Central Analytical Facilities (CAF), NMR unit, Stellenbosch University, Schumann Annex De Beer Street, 7600 Stellenbosch, South Africa

<sup>e</sup> Politecnico di Bari, DMMM, Via Re David 200, 70125 Bari (BA), ITALY

<sup>f</sup> AC BOILERS S.p.A, Largo Buffoni n°3, 21013 Gallarate (VA), ITALY

### Abstract

The present paper describes the steps followed to develop a detailed and reliable combustion modelling procedure whose application as major engineering design tool supported *AC-Boilers* (ACB), a major Italian boiler manufacturer, in routing its products development to highly efficient burners for power generation purposes, while adopting a significantly reduced time to market. In 2018, in the frame of the R&D project named *BE4GreenS* supported by *Regione Puglia*, a technical partnership between ACB, *Centro Combustione Ambiente* (CCA) and *Politecnico di Bari* has been set-up to expand the expertise of ACB and CCA in burner design and full-scale testing to the numerical modelling field. The partnership led to the creation of an R&D team, named *Energy Transition to the Future* (ETF), made by engineers and scientists with expertise in numerical modelling and combustion phenomena. The ETF group has been working on the design and numerical testing of highly innovative low-emission burners by using CFD as a design tool rather than a merely investigation tool. The first milestone of the working plan consisted in the definition of a three-flux low-NO<sub>x</sub> 35MW clean coal burner. The design process started with the definition of the design principles to be followed along with the coal and flame pattern to be achieved. Once pinpointed the first geometries to be tested, those were investigated through detailed CFD studies and optimized in terms of pollutants emission and flame stability. Each burner geometry was numerically tested including in the numerical domain the actual CCA 48MW combustion chamber volume, the windbox and the OFA ports to avoid any airflow assumption. The actual extension of the heat exchanging and refractory surfaces of the combustion chamber was also added to the numerical domain for its completeness. The fuel to be used was in-deep characterized by the *Istituto di Ricerche sulla Combustione* (IRC), the *Ruhr-Universität* (LEAT), and the *Central Analytical Facilities* (CAF), NMR unit. The application of coal specific data allowed to define highly detailed coal devolatilization and burnout models. Two different burners were experimentally tested at CCA plant along with the previous ACB 35MW market burner (TEA-C) for benchmark. The experimental test shed light on the excellent performance of the prototypes in terms of efficiency (significant abatement of unburnt carbon), emissions (highly reduced NO<sub>x</sub> and CO production with limited air excess) and flame stability (below 50% coal full firing load achieved with less than 5% of unburnt carbon). Also, the remarkable agreement observed between predicted and measured data triggered the scale-up process of the 35 MW burner to different sizes (45 MW, 55 MW and 65 MW) through the definition and CFD test of specific scaling laws. The ETF working plan foresees the definition of a set of different multi-fuel burners (coal, oil, gas, biomass) in different sizes within the challenging 3 years time span. Details of steps followed during the design and testing process of 35MW prototypes are herein provided.

### Introduction

In the last decades, significant efforts have been made to develop cleaner and more efficient technologies to control Greenhouse gases (GHG) emissions [1]. Nonetheless, the current rate of progress is far from sufficient to reach the carbon output reduction target agreed during the 2015 United Nations Climate Change Conference (COP 21) [2]. The discussed mitigation pathway requires,

in fact, huge investments and a fast pace of technological progress from both the industrial and academic community. The present paper describes how the employment of CFD modelling as major engineering design tool supported *AC-Boilers* (ACB) in routing its products development to highly efficient burners for power generation purposes while adopting a significantly reduced time to market. The Computational Fluid Dynamic (CFD) is a branch of physics widely recognized as a powerful tool to gain insights into problems involving fluid flows. The use of numerical techniques, coupled with detailed modelling of thermodynamic, chemical kinetics and fluid mechanics allows to accurately predict highly turbulent flows patterns within full-scale industrial boilers. This is particularly true with the recent progress in High Performance Computing (HPC) which allows for a high level of complexity of the burner geometries investigated [3], [4]. The production of trustworthy data allows more design variations to be studied numerically while cutting down the number of full-scale tests. This leads to a shorter design cycle and the product development cost reduction.

Despite numerical modelling is broadening its application as an engineering design booster, experimental tests will continue to play a major role in the burner performance assessment, numerical design validation, burner commissioning activities and, particularly, by providing valuable data set to CFD engineers to improve the numerical model accuracy. In 2018, in the frame of the R&D project named *BE4GreenS* supported by *Regione Puglia*, a technical partnership between ACB, *Centro Combustione Ambiente* (CCA) and *Politecnico di Bari* has been set-up to expand the expertise of ACB and CCA in burner design and full-scale testing to the numerical modelling field. The partnership led to the creation of an R&D team, named *Energy Transition to the Future* (ETF), made by engineers and scientists with expertise in numerical modelling and combustion phenomena. The ETF group has been working on the design and numerical testing of highly innovative low-emission burners by using CFD as a design tool rather than a merely investigation tool.

Following a continuous know-how transfer between ACB, CCA and ETF groups the definition of the detailed design of two different 35MW burners was targeted in significantly less than one year. Both burners were experimentally tested at CCA plant along with the previous ACB 35MW market burner (TEA-C) for benchmark. Hereafter prototypes are named as *BE4G-35-1* and *BE4G-35-2* or, without distinction, *BE4G-35*. The experimental test shed light on the excellent performance of the prototypes in terms of efficiency (significant abatement of unburnt carbon), emissions (highly reduced NO<sub>x</sub> and CO production with limited air excess) and flame stability (below 50% coal full firing load achieved with less than 5% of unburnt carbon). Also, the remarkable agreement observed between predicted and measured data triggered the scale-up process of the 35 MW burner to different sizes (45 MW, 55 MW and 65 MW) through the definition and CFD test of specific scaling laws.

### **BE4G-35 Design Principles**

The BE4G-35 burner has been designed aiming to a drastic emission reduction with respect to the TEAC burner while improving the TEAC overall efficiency.

The design activities were initially routed to the Nitrogen Oxides (NO<sub>x</sub>) reduction (hard coal firing) through the achievement of an effective separation of the Primary Air (PA or transport air) from the Secondary Air (SA) and Tertiary Air (TA), and, equally important, through the achievement of early stages of ignition (pyrolysis and volatile oxidation) in the Near Burner (NB) region (flame holder area). With the achievement of optimized air separation, a fuel-rich region in the NB area follows. The start of the ignition process in the NB area causes coal Volatile Matter (VM) to be released under low oxygen conditions, in such a way that nitrogen oxides formation from fuel bounded nitrogen (N<sub>2</sub>) is hampered and nitrogen compounds (NO<sub>2</sub>, NO, N<sub>2</sub>O) reduction to N<sub>2</sub> is promoted. Significant efforts have been made to create a stable self-ignition over a wide burner load range. The BE4G-35 burner features an axisymmetric design with swirled PA, SA and TA flow streams to obtain a uniform and stable Internal Recirculation Zone (IRZ). The burner geometry has been optimized to force the recirculation zone back to the flame holder device (i.e. the ignition area). The presence of a teeth ring at the coal pipe end slow down the coal particles enough to achieve backfire. As a result, ignition occurs at teeth ring and the resulting hot exhaust gases are entrained in the recirculation flow, back to flame holder. The hot oxygen lean back-flow self-sustain the devolatilization process assuring an extremely stable flame. The BE4G-35 burner has been designed to provide a sufficient amount of PA to initiate and self-sustain the ignition process of pulverized hard coals with a volatile content ranging typically from 20% to 50%. The SA and TA register has been designed to progressively feed the char burnout process once volatile is mostly released and consumed.

The reduction of unburnt carbon (UBC) left in ashes was another major field of improvement targeted during the BE4G-35 design process. To reach the target, the design activities were focused to an effective mixing and segregation of the pulverized fuel along the primary duct. An optimal mixing plays a major role in the achievement of an axisymmetric and well-controlled flame, while optimal

segregation guarantees that the bulk of Pulverized Fuel (PF) is guided against teeth. The two prototypes manufactured differs only in internal devices used to achieve segregation and mixing. The BE4G-35-1 is equipped with an S-shaped elbow, a deflecting plate and a bluff-body with built-in swirler to achieve the PF mixing and segregation (Figure 1a).

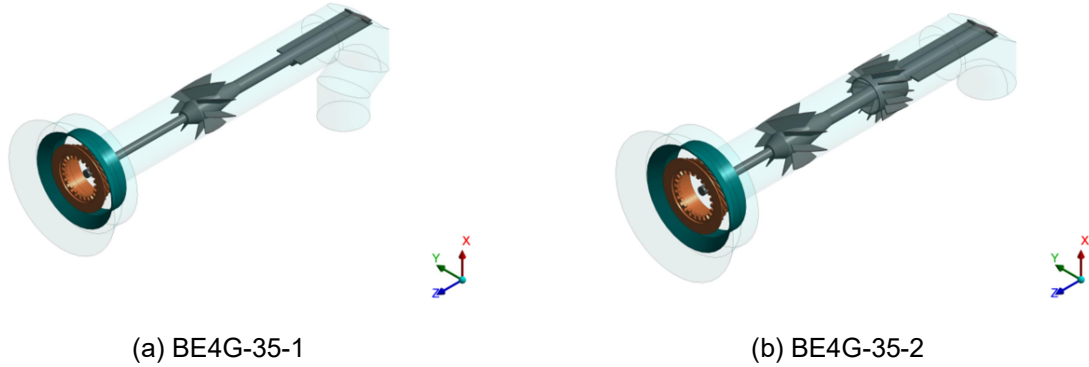


**Figure 1.** Isometric view of the BE4G-35-1 (left) and BE4G-35-2 (right). The figure highlights the S-shaped elbow, the deflecting plate, the bluff-body with the built-in swirler, the coaxial counter swirler and the nozzle.

Conversely, the BE4G-35-2 features a standard elbow, a deflecting plate, a Coaxial Counter Swirler (CCS) and a bluff-body with built-in swirler to achieve the PF mixing and segregation (Figure 1b). The BE4G-35 design process also aimed to improved control of the combustion air (Air from windbox) distribution. The air from windbox, once split into SA and TA through the air register, plays a major role in controlling the flame shape (mainly through the TA), controlling NO<sub>x</sub> formation (mainly through the SA), and oxidizing the char through staged combustion.

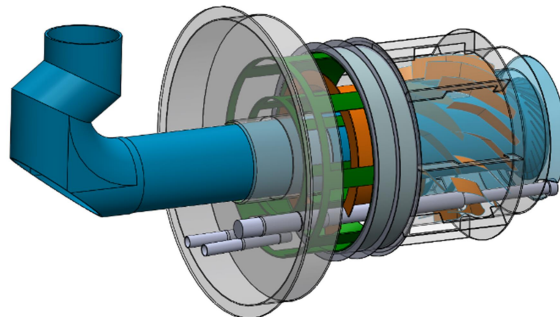


**Figure 2.** Isometric view of the BE4G-35-1 burner coupled with the secondary and tertiary air register.

As such, an optimal balance between SA and TA was targeted to reach both a significant flame control and low emissions. In addition, a wide rangeability of the SA/TA ratio was targeted to guarantee flame control and low emissions over a large set of firing conditions. Both BE4G-35 prototypes were equipped with a newly designed air register capable to operate over the 0.5-0.7 SA/TA ratio (design range) regardless of the general air damper position. The air register design guarantees that, within the 0.5-0.7 SA/TA range, the air axial velocity upstream the SA cone and TA quarl remains below 30m/s (approximately 25m/s with SA/TA equal to 0.6). Moreover, the new air register allows a 30°-60° swirl range for both SA and TA. A 3D render of the BE4G air register is shown in Figure 2.

## Numerical Model

The objects of the CFD study were both the full-scale BE4G prototypes and the CCA combustion chamber, wherein the burners were experimentally tested. The numerical domain consists of the primary air duct (entirely modelled), the secondary and tertiary air ducts (entirely modelled), and the combustion chamber (entirely modelled).

The origin of the computational domain coordinate system lays at the centre of the combustion chamber inlet, with the burner and the CC horizontally displaced along the z-axis. To achieve numerical results as much accurate as possible and to limit the maximum number of cells, a hybrid multi-block approach was used. As such, finer grids were applied where stronger gradients (e.g. around the swirler, at the burner outlet, etc.) were expected. The entire 3D geometry was meshed with approximately  $4 \cdot 10^6$  polyhedral cells. Polyhedral cells were preferred to hexahedral ones to avoid any directionality in the mesh pattern, which could potentially route flows along a preferred solution. Despite the complexity of the burner geometry, numerical grids of both prototypes presented a skewness lower than 0.77.

The boundary/inlet conditions have been set as follows: coal dry particle mass flow rate,  $G_{PC} = 1.141$  kg/s at  $T_{PC} = 350$  K (LHV DAF = 34 MJ/kg for a total thermal input of 35 MW); primary air mass flow inlet,  $G_{a1} = 2.283$  kg/s at  $T_{a1} = 350$  K; Total air mass flow rate,  $G_T = 11.64$  kg/s at  $T_T = 564$  K (resulting in a combustion excess air of approximately 17%). Concerning the heat transfer boundary conditions, different materials are employed throughout the combustion chamber surfaces modelled with an overall heat transfer coefficient ranging from 3.8 to 28.3 W/(m<sup>2</sup> K) and internal emissivity 0.4, whereas the overall heat transfer coefficient is 5000 W/(m<sup>2</sup> K) for evaporator walls, considering a 485 K free stream temperature and a 0.5 internal emissivity. The continuous phase flow is computed by solving the Reynolds Averaged Navier Stokes (RANS) equations, with a 2-equations realizable k- $\epsilon$  model for turbulence closure, discretized according to a finite volume approach. Non-equilibrium wall functions have been used for the near-wall treatment of turbulence.

Combustion in continuous phase has been modelled by the non-premixed combustion approach employing a single fuel stream and an oxidizer stream with a single mixture fraction  $Z$  describing the mixture composition and a probability density function (PDF) to take into account reactions and turbulence-chemistry interaction. PDF look-up tables have been computed for a twenty species mixture, from which, given the enthalpy, the mixture-fraction and its variance, all the gas-mixture thermodynamic and transport properties (density, constant pressure specific heat capacity, molecular viscosity) can be evaluated. Sutherland's viscosity law has been considered in order to deal with the molecular viscosity dependency on temperature, while for the continuous phase density an ideal gas state equation has been assumed such that it depends on temperature while it is independent of the local pressure (incompressible model with constant bulk pressure).

**Table 1.** Coal-specific CPD parameters for New Glory coal (CNR analysis)

Parameter	Symbol	New Glory	Unit
Initial fraction of bridges in the coal lattice	$p_0$	0.636	-
Initial fraction of char bridges	$C_0$	0	-
Lattice coordination number	$\sigma+1$	5.695	-
Cluster Molecular Weight	$MW_l$	537.338	kg/kmole
Side Chain Molecular Weight	$MW_\delta$	44.67	kg/kmole

**Table 2.** Proximate and Ultimate analysis for New Glory coal (CNR analysis)

	Proximate Analysis (weight % as received basis)				Ultimate Analysis (weight % as received basis)				
	Ash	Volatile	Char	Moist.	C	H	O	N	S
New Glory	9.60	38.06	50.43	1.91	74.09	5.11	7.00	1.48	0.81

The pulverized coal has been treated as a discrete phase and modelled through a two-way coupling Lagrangian approach. The collisions of the coal particles with the burner walls and internals have been treated as elastic while an inelastic (no-bounce) condition has been assumed for collisions with the combustion chamber walls. The particle distribution at the domain inlet and the coal characteristics are based on the pulverized coal used in the previous experimental test. The pulverized coal was milled and then classified by means of a rotating sieve at 200 rpm (99.63% with  $d < 300$   $\mu\text{m}$ , 98.37% with  $d < 150$   $\mu\text{m}$ , 87.88% with  $d < 75$   $\mu\text{m}$ ), obtaining a diameter distribution well approximated by a Rosin-Rammler distribution with the following parameters: minimum diameter of 5  $\mu\text{m}$ , maximum diameter of 150  $\mu\text{m}$ , mean diameter of 50  $\mu\text{m}$  and spread parameter of 1.5. The discrete solid-phase enters the

domain by a uniformly distributed injection from the primary air inlet, divided into 74400 parcels obtained as the number of faces (744) multiplied by the number of diameters considered in the Rosin-Rammler distribution (20) multiplied by the number of turbulent tries (5) for each stream.

Radiative heat transfer has been accounted for by means of the DO (Discrete Ordinate) model, solving the Radiation Transfer Equation with a Finite Volume discretization on a discrete number of directions. A domain-based Weighted-Sum-of-Gray-Gases Model (WSGGM) approach has been used to derive the absorption coefficient in the continuous phase. Particle-gas radiation interaction has been taken into account, assuming particle emissivity of 0.9 and scattering coefficient equal to 0.6 [5].

The pulverized coal combustion process is split into the following steps: (i) particle heating; (ii) devolatilization; (iii) volatile matter combustion (homogeneous combustion in the continuous phase); (iv) char burnout (heterogeneous combustion on the particle surface releasing CO<sub>2</sub> in the gas phase). The inert heating laws are applied when the particle temperature is lower than the assigned devolatilization temperature. The devolatilization law is applied when the temperature of the particle reaches a temperature of 650 K, until the mass of the particle, exceeds the mass of the non-volatiles in the particle. The moisture content of coal particles and the particle swelling during the devolatilization process have been neglected.

The Chemical Percolation Devolatilization (CPD) model has been employed to describe the devolatilization process under rapid heating conditions. It considers the thermochemical transformations of the coal structure rather than using empirical relationships [6]. As such, input data required by the CPD model (5) are coal-specific, obtainable employing solid-state <sup>13</sup>C Nuclear Magnetic Resonance (four coal lattice parameters out of five calculated) and a simple empirical relations (C<sub>0</sub> parameter) function of the coal rank. For the present study, the initial fraction of char bridges (C<sub>0</sub>) has been set to zero, which is a typical value for bituminous coals [7]. The CPD parameters (see Table 1) have been supplied by the Central Analytical Facilities (CAF) of Stellenbosch University - South Africa, as a result of Solid-State <sup>13</sup>C NMR analysis on a New Glory coal sample, the same fuel burned during the experimental test. A detailed description of the NMR characterization is provided in "Fuel Characterization" section. For the sake of completeness, the proximate and ultimate analyses are reported in Table 2.

The char burnout model used considers coal as made by porous spherical grains. Every grain may be described by a carbon matrix with the remaining chemical elements and the inert mineral phase defined by the ultimate analysis, uniformly distributed. The combustion law, here considered, consumes the reactive content of particle following a heterogeneous reaction. The Intrinsic char burnout model used for the present CFD study computes the heterogeneous reaction rate considering both kinetics and O<sub>2</sub> pore diffusion phenomena. The Intrinsic model input data used are summarized in Table 3.

**Table 3.** Kinetic/diffusion-limited surface reaction rate parameters for New Glory coal (CNR analysis)

Parameter	Symbol	New Glory	Unit
Mass Diffusion-Limited Rate Constant	C <sub>l</sub>	5·10 <sup>-12</sup>	-
Kinetic-Limited Rate Pre-Exponential Factor	A <sub>i</sub>	0.000106	-
Kinetic-Limited Rate Activation Energy	E <sub>i</sub>	1.23·10 <sup>8</sup>	Joule/kmole
Char Porosity	θ	0.4	-
Mean Pore Radius	r <sub>p</sub>	5·10 <sup>-9</sup>	m
Specific Internal Surface Area	A <sub>g</sub>	309000	m <sup>2</sup> /kg
Tortuosity	τ	1.5	-
Burning Mode	α	0.25	-

In order to predict NO<sub>x</sub> emissions, a transport equation for nitric oxide (NO) concentrations has been solved. The NO<sub>x</sub> formation has been evaluated according to the thermal and fuel-NO mechanisms; hence, two additional transport equations for intermediate species (HCN and NH<sub>3</sub>) have been considered. The NO<sub>x</sub> transport equations are solved in post-processing based on frozen flow fields and combustion solutions. The formation of thermal NO<sub>x</sub> is determined according to the extended Zeldovich mechanism, and the rate constants have been selected based on the evaluation of Hanson and Salimian [8]. The needed concentrations of O, H and OH is derived from temperature and O<sub>2</sub> and H<sub>2</sub>O concentrations by means of a heuristic relation. Organic compounds present in coal and containing nitrogen can significantly contribute to the total NO<sub>x</sub> formed during the combustion process. Fuel nitrogen is split between volatiles and char during coal devolatilization and in the nitrogen conversion can originate hydrogen cyanide (HCN) and/or ammonia (NH<sub>3</sub>). Local NH<sub>3</sub> and HCN

concentrations derive from the solution of the respective transport equations solved in post-processing according to the kinetics developed by De Soete [9]. The nitrogen contained in the char is heterogeneously oxidized to NO via an overall reaction.

The entire set of input data required by the Intrinsic model, along with the char nitrogen content and the HCN/NH<sub>3</sub> partition were provided by the Istituto delle Ricerche sulla Combustione (IRC) of Naples following a New Glory sample characterization. The whole set of data is New Glory coal specific. A more detailed description of the aforementioned characterization is provided in "Fuel Characterization" section.

## Fuel Characterization

The BE4G-35 prototypes and the TEA-C burner were experimentally tested at CCA plant, all burners fueled with a bituminous Colombian coal named *New Glory*.

The Input coal lattice parameters required by the CPD model to characterize the coal devolatilization process were experimentally obtained through two specific Solid-State <sup>13</sup>C NMR experiments. A New Glory coal sample was submitted to the *Central Analytical Facilities* - South Africa for this solid-state NMR characterization. The solid-state NMR spectra were acquired on a Wide Bore Agilent VNMRS 500 MHz two-channel spectrometer using zirconia rotors and a 4 mm Chemagnetics™ T3 HX MAS probe. Magic-angle-spinning (MAS) was performed at 12 kHz and Adamantane was used as an external chemical shift reference standard, where the methyl peak was referenced to 38.4 ppm. All cross-polarization (CP) spectra were recorded at 25°C with proton decoupling, a relaxation delay of 3s and 10000 transients are collected for adequate signal-to-noise. The power parameters are optimized for the Hartmann-Hahn match and the radiofrequency fields are equal to CB1C=HB1H≈58kHz. The chosen contact time for cross-polarization was 2ms. The free induction decay (fid) recorded 3500 points with each transient. After completion, the combined fid is Fourier transformed with a 125 Hz line broadening. The dipolar dephasing experiments are carried out under similar conditions with the interrupted decoupling time constant, t1Xidref set to 40us after evaluating an array of time constants. All experiments were performed with the same receiver gain setting and number of transients, with identical acquisition parameters.

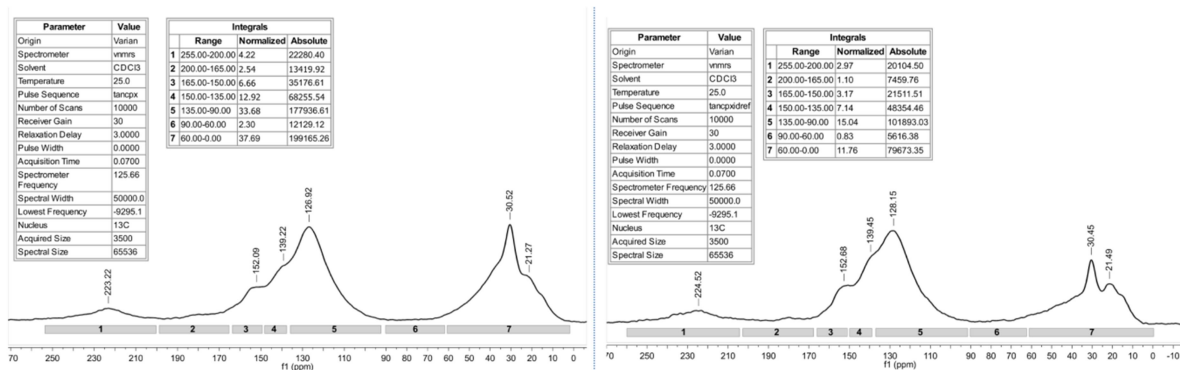


**Figure 3.** <sup>13</sup>C CP-MAS spectrum of a New-Glory coal sample (left). <sup>13</sup>C CP-MAS with Dipolar Dephasing spectrum of a New-Glory coal sample (right)

In Figure 3 the coal sample spectra with integral reset points of the <sup>13</sup>C CP-MAS and Dipolar Dephasing experiments are shown. These integration reset points and calculations are adopted from Solum *et al.* [10], [11]. The licensed Mestrenova 12.0.2 software package was used to process the spectra and an integral reset table created in order to ensure that exactly the same regions are integrated reproducibly. The spectra are each phased and baseline corrected manually before integration. All spectra were processed in the same manner and at the same time to minimize operator bias. The integral values are transferred to a prepared Microsoft Excel spreadsheet for calculation of the coal structural parameters as per the published literature [10], [11]. No Variable Contact Time (VCT) experiments are employed for this method, mainly because of long acquisition times [10], [11]. A contact time of 2μs was used for all experiments as a compromise. A correction factor of 1.3 as derived from literature was used to correct the intensity of the bridgehead aromatic carbons (peak 135-90ppm for dipolar dephasing experiment) for the loss in magnetization during the interrupted decoupling [10], [11], [12], [13].

In addition to CPD input data, a large array of experimental determinations has been carried out to measure all the input data required by the intrinsic pore model and the NO<sub>x</sub> model. Those data follows

the characterization of coal, its pyrolysis and combustion behaviour. A New Glory coal sample was submitted to the IRC - Italy for characterization.

Proximate and ultimate analyses were carried out according to ASTM 5142 ed ASTM D5373 procedure, the high heating value was calculated by Isoperibolic calorimeter Parr 6200. Pyrolysis behaviour has been preliminarily investigated by thermogravimetric analyses using a NETZSCH 409 TGA DSC apparatus. Approximately 20 mg of sample was loaded into the sample pan for each test and heated from 110 to 850°C at 5°C/min in a 250 ml/min flow of nitrogen.

Coal has been pyrolysed at Bochum University under fast heating conditions using a Drop Tube Reactor (DTR). Pyrolysis was carried out at 1300°C in nitrogen and char was sampled with a residence time of 0.05 s. Prior to pyrolysis in the DTR the coal sample was ground and sieved. Its granulometric analysis was carried out by Mastersizer 2000 laser granulometer (Malvern Instruments) and a mean volumetric diameter of 130  $\mu\text{m}$  was measured. DTR char particles are approximately spherical and have a rather smooth surface, as can be appreciated from

Figure 4. Their morphology suggests that they have passed through a plastic stage. Some submicronic particles are also observed, which can be ascribed to soot or to fragmented char. Excluding these finer particles, the mean volumetric diameter of the collected char, measured by the laser granulometer, is 142  $\mu\text{m}$ , which compared with the value of the raw coal allowed to estimate the swelling coefficient (1.1).

The char sample was oxidized in air at 400°C to remove traces of residual volatile matter and to open up closed porosity. Then it was subject to a train of porosimetric analyses: the true density was measured by a suspension magnetic balance Rubotherm type IsoSORP in Helium at ambient temperature and 0-20 bar. Nitrogen adsorption at 77K was carried out in a Quantachrome Instrument. Mercury intrusion porosimetry was carried out by means of an AutoPore IV 9500.

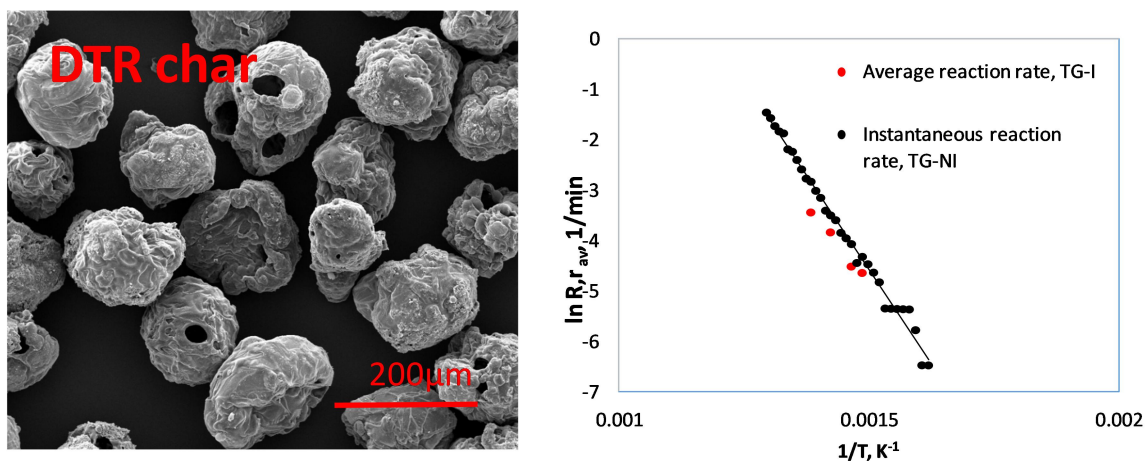


**Figure 4.** SEM picture and combustion reactivity of DTR char measured by TGA [14] [15]

Intrinsic kinetics of char combustion has been described through a first-order kinetic law. The pre-exponential factor and activation energy have been evaluated by means of thermogravimetric analysis. The experimental campaign was carried out in a NETZSCH 409 TGA DSC and included both non-isothermal and isothermal tests. In each test, approximately 20 mg of sample was loaded in the pan. In non-isothermal runs, the sample was heated up from 110°C to 850°C at 5°C/min in a 250 ml/min flow of air. In isothermal runs, the sample was heated at 50°C/min up to the set temperature TR in a flow of nitrogen, before the gas is switched to air. The set temperature TR varied between 350-550°C. The mass loss data were worked out to calculate the instantaneous rate of carbon conversion (R) versus time and the conversion rate averaged over the first 50% (raw). Results have been used to calculate Arrhenius plots of the instantaneous and of the average combustion rate vs.  $1/T$  (

Figure 4). Regression analysis over the linearity range of the plots, allowed to estimate the pre-exponential factor  $A_i$ , and activation energy  $E_i$ .

### Numerical Test

As mentioned in the "Introduction" section, more burner geometries were numerically tested before promoting BE4G-35-1 and BE4G-35-2 to the final test phase. As such, a number of different studies

were performed. Those involving either reacting and non-reacting flows. Similarly, more boundary conditions were used as "numerical stress tests" to gain insights into the flow patterns within PA, SA, TA, OFA ducts and the combustion chamber.

For reacting flows studies, the numerical solution has been considered converged when all of the following conditions were reached:

- The flue gas temperature evolution at the cc exit oscillate around a constant value;
- The sensible and formation enthalpy net balance in the whole domain (~ 50 kW) is negligible with respect to the TEA-C thermal power (~ 35 MW);
- The evolution of the solution residuals presents a flat profile when compared with the previous DPM source update.

Following the mentioned conditions, the "hot cases" reached the numerical convergence after approximately 12000 iterations. As a rule of thumb, the first 2000 iterations were run without considering the interaction between the discrete and continuous phase. The PDF transport and the DO equations were disabled. The following 1000 iterations were run with the Discrete Phase Model (DPM) enabled, while keeping the PDF transport and the DO equations disabled. The following iteration was run with the temperature patched at 1500 K in a defined cylindrical volume in the near burner region. The remaining iterations were run activating also the PDF transport and the DO equations.

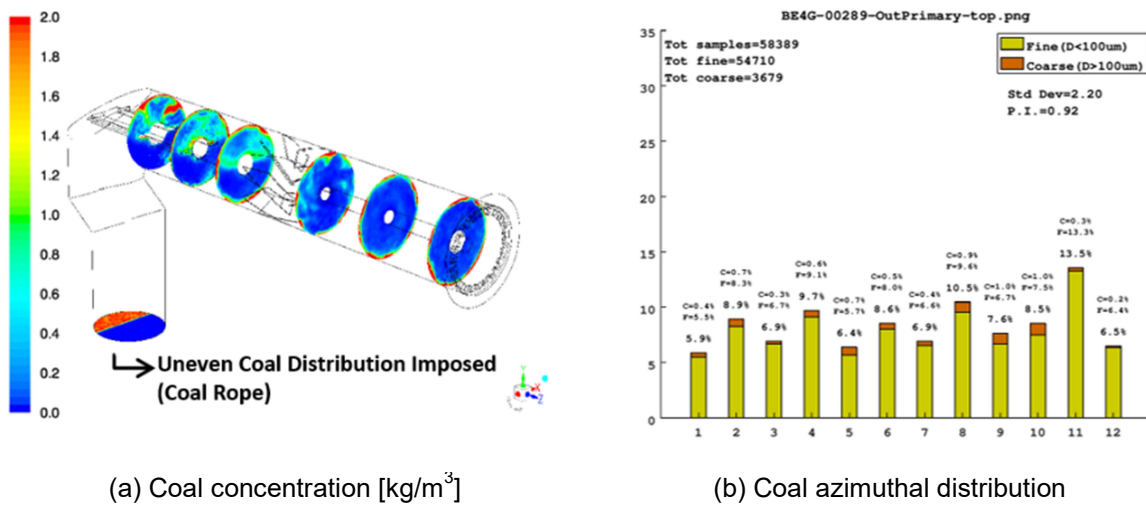


**Figure 5.** Left: coal concentration along the primary air duct of the BE4G-35-1 burner. Right: coal parcels count in twelve different sectors taken on a control surface upstream the teeth-ring. The bar chart diagram is obtained by means of an ACB in-house code.

In Figure 5a the concentration of coal along the primary air duct is shown when a strong uneven distribution is forced to flow at the burner inlet. As the figure clearly shows, the particular geometry of the S-shaped elbow, coupled with all the internal devices, generates an isotropic non-homogeneous coal distribution immediately before the teeth-ring. Going into more detail, the coal flow pattern results properly mixed downstream the swirler, while concentrated along the internal PA duct surface.

The qualitative insights from the coal concentration contour are confirmed by quantitative observation when the number of coal parcels (either fine and coarse parcels) are counted along twelve different azimuthal sectors in a section upstream the teeth-ring. The parcel count is obtained through a specifically developed ACB in-house code. As Figure 5b describes, each bar in each sector presents a comparable height (either yellow and orange regions), which is a remarkable result considering the tough boundary condition at the inlet. Because of the peculiar coal distribution upstream the burner outlet, coal particles are forced to collide against the teeth-ring, reducing significantly their velocity. As a result, a backfire process is triggered and ignition occurs at the teeth-ring. It is worth noting that a second complex numerical algorithm (ACB proprietary) has been specifically developed to calculate the proper dimensions of the nozzle as a function of the fuel density and granulometry to assure the fuel/teeth-ring collision.

The BE4G flame pattern is well described by Figure 6b, where the contour of T in the cross-section area along the burner axis is zoomed in the near burner region. The figure confirms the generation of a red hot region at the teeth-ring, where ignition takes place. Two green bulges can also be observed

in the figure. These areas suggest the presence of a recirculation pattern downstream the teeth-ring. The presence of a recirculation area is confirmed by the contour of the axial velocity (Figure 6a) when only positive values are plotted and negative values are clipped. Here two white region in proximity of the teeth-ring can be observed, demonstrating the generation of flow patterns back the burner nozzle. It is interesting to note that the backflow mainly entrains hot flue gases (Figure 6c). This helps the self-sustainment of the flame in an oxygen lean region, assuring an extremely stable flame. In addition, the release of volatile matter in this area (Figure 6d) promotes reduced emission as the Nitrogen oxidation is hampered by the low oxygen content. Moreover, as flue gases flow back, part of the coal particles remain entrained in the recirculation pattern (Figure 6e) increasing their residence time. As a result, insights from CFD studies suggest a strong abatement of emissions and a highly improved flame stability (see next section).

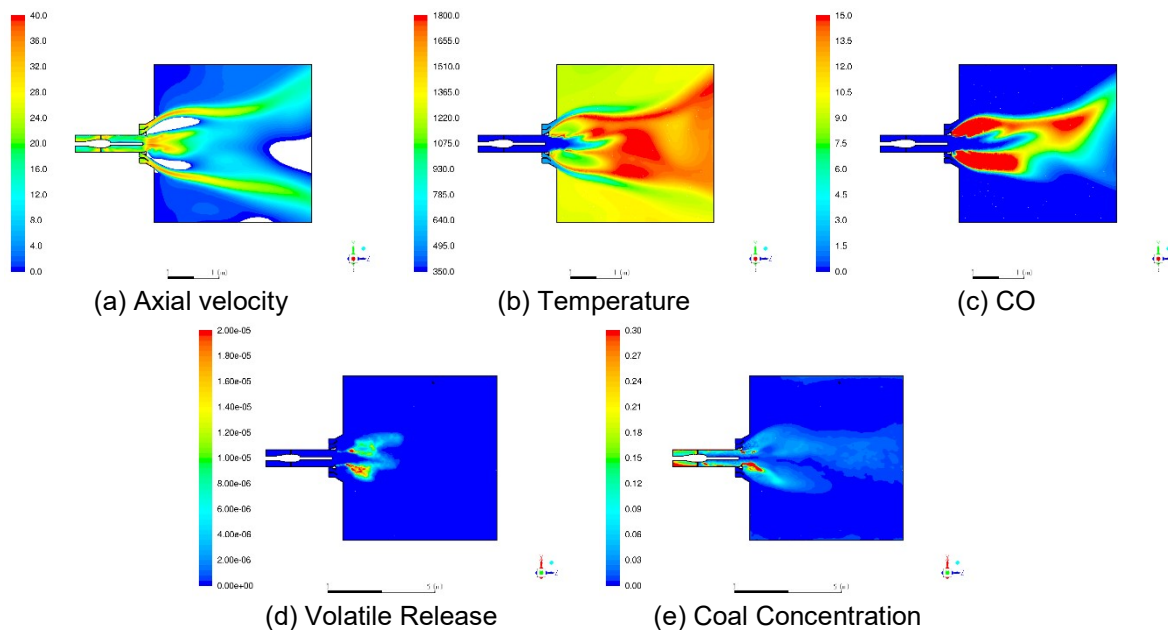


**Figure 6.** Top left: Axial velocity contour [m/s] in the NB region. White areas are clipped to negative values. Top middle: temperature contour [K] in the NB region. Top Right: CO concentration contour [Vol% dry] in the NB region. Bottom left: Volatile release rate [kg/s] in the NB region. Bottom right: Coal concentration [kg/m<sup>3</sup>] in the NB region.

### Experimental Test and CFD validation

The CCA facility consists of multiple test areas each equipped with cutting edge measurement devices, supporting a wide range of experimental applications either performed with gaseous (e.g. natural gas, hydrogen, carbon monoxide, etc.), liquid (light fuel oil, heavy fuel oil, etc.), or solid-state fuels (coal, biomass, solid recovered fuel, etc.).

The BE4G-35 prototypes and TEA-C burner were all installed and operated as a stand-alone configuration in the 48MWth CCA combustion chamber. The combustion chamber is approximately 5.5m high, 4.35 m wide and 12.5 long. It presents four Over Fire Air (OFA) ports and ten windows displaced along the burner axis for in-flame probes insertion. Windows 3, 4, 5, and 6 (1.181, 1.562, 2.095 and 2.628 m respectively away from burner inlet) were selected for the experimental in-flame measurements and numerical/experimental data benchmark. It also features a bottom hopper with a dry ash extraction system. A sketch view of the BE4G-35-1 burner along with the cc volume and the location of the selected in-flame measurement windows is shown in Figure 7. Downstream the combustion chamber, the flue gas flows through the convective bank at the rightmost side of the boiler, where part of the total steam produced is superheated. The inner cc surface is partly refractory coated. An airfoil flow meter is used to measure the airflow through the burner windbox. A second airfoil flow meter is used to control the mass flow rate of the excess air through the OFA ports. In addition, each BE4G-35 air register is equipped with two Pitot rings (static and total pressure) to accurately measure and control the SA/TA air ratio. The air mass flow rate through the primary duct is instead measured by means of an Annubar averaging Pitot, previously characterized. The control of the pulverized coal mass flow rate is obtained by setting the number of revolutions per minute of the

pulverized coal feeding system. The mass flow rate dependence to the number of revolutions per minute has been previously characterized storing the pulverized coal on a balance, with density verification. Two EUcoalflo<sup>TM</sup> sensors are also installed downstream the mill to assure redundancy of the fuel flow measure. Moreover, the coal flow rate is numerically estimated through an ACB in-house developed code.

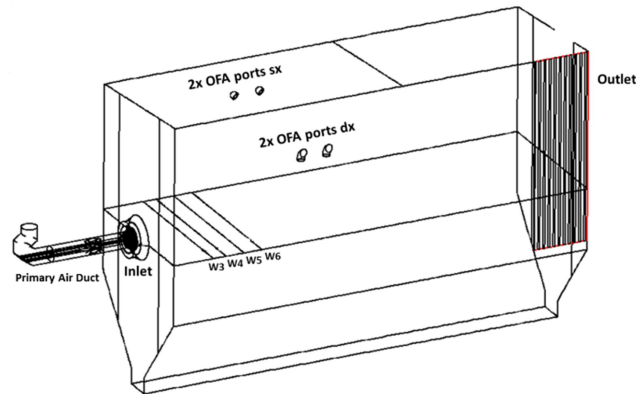


**Figure 7.** Isometric sketch view of the BE4G-35-1 burner installed in the 48MWth CCA combustion chamber. The air registers are not shown.

To perform the flue gas analysis, four different units were used. The flue gases are sampled from a grid located upstream the air heater and directly conveyed (via a heated probe) to the analyzer. The grid is composed of four probes, each ending with a silicon carbide filter. Two suction-type pyrometers, one equipped with a K-type thermocouple and the second with a B-type thermocouple, are placed at the combustion chamber exit for flue gas temperature evaluation. The in-flame measurements were performed via a suction-type pyrometer equipped with an S-type thermocouple. The thermocouple has two head shields, the outer one made of titanium alloy, whereas the inner one in alumina. Once placed in position, the pyrometer sucks in the bordering gases through steam ejection. The sampled gases were analyzed by means of two portable analyzers. The data acquisition system is designed with a commercial programming environment according to ACB testing needs.

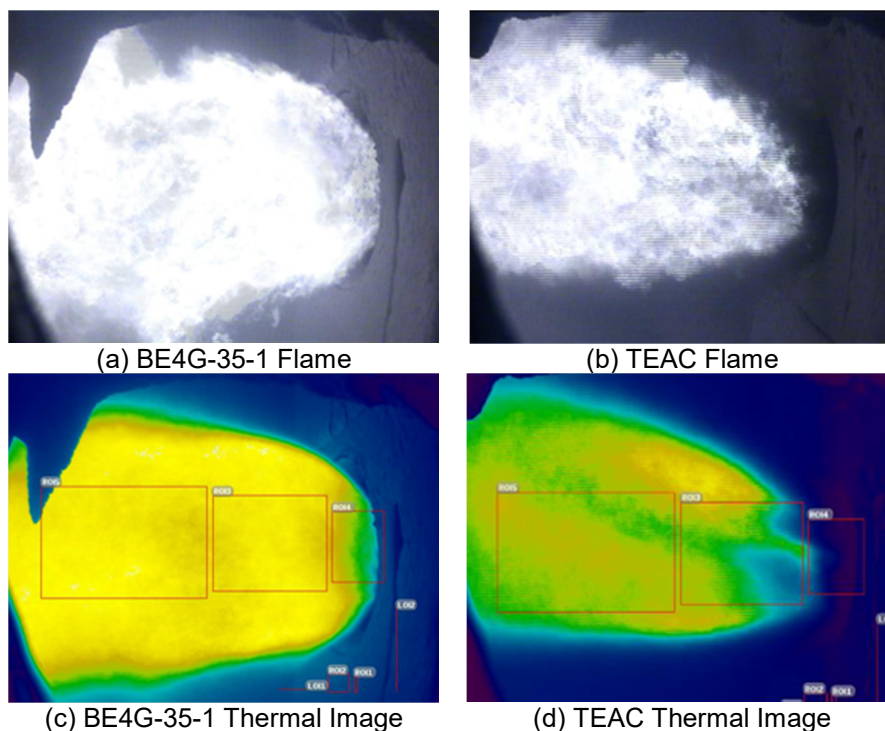


**Figure 8.** BE4G (left column) and TEAC (right column) flame pattern in the near burner region at coal full-firing load captured by the thermal camera.

The experimental test shed light on the excellent performance of both prototypes in terms of flame stability, emissions and efficiency. The differences in the flame pattern behaviour between TEAC and BE4G prototypes are described in Figure 8 where images from the thermal camera are shown. The BE4G prototypes both highlighted a wide hot flame root entirely attached to the burner nozzle, as predicted by CFD investigation. Conversely, the TEAC flame evidenced a mildly irregular flame pattern, detached from the burner nozzle. When operated at partial load (below 50% of the full firing coal load), both BE4G burners showed the same flame pattern with a significantly low amount of unburnt carbon (less than 5%) and no clues of a starting flame extinction process.

The encouraging performance improvement of the new BE4G burners depicted from CFD analysis was also observed during the experimental test, which also highlighted a big step ahead of new burners with respect to the previous one in terms of efficiency (UBC) and emissions (NO<sub>x</sub>, CO).

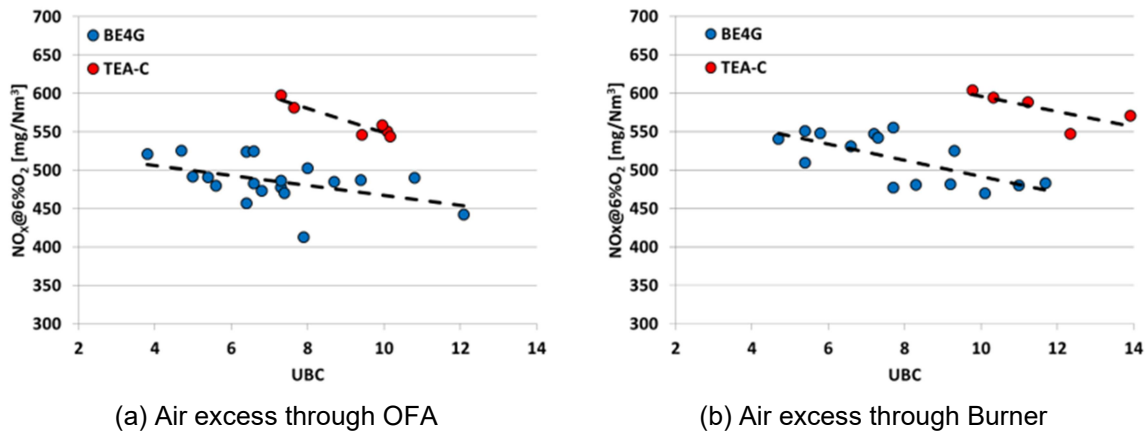


**Figure 9.** TEAC (red dots) and BE4G (blue dots) emission performance benchmark. The figure on the left refers to burners operating in stoichiometric conditions. The figure on the right refers to burners operating with stoichiometry equal to 1.2.

On Figure 9 the emission performance of the BE4G-35-1 burner is compared to the performance of the TEAC burner. Both burners were operated in stoichiometric conditions (left figure) and with stoichiometry equal to 1.2 (right figure). When operated in stoichiometric conditions, the air excess flows through the OFA openings. Conversely, the air excess flows through the windbox. The total stoichiometry was kept constant to 1.2 over the entire test campaign. As the figures show, in both cases, the blue dots remain well below the red ones over the entire range explored. When compared to the TEAC burner, the benchmark particularly sheds light on the BE4G NO<sub>x</sub> reduction higher than 20% and the UBC reduction higher 40%. It is worth noting that BE4G performance is even more remarkable if referred to the relatively small volume of the test combustion chamber. In absolute terms (industrial plants), significantly lower emissions are expected.

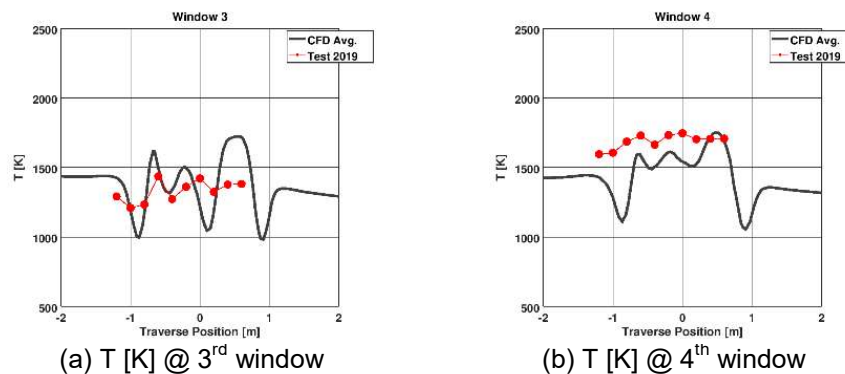


**Figure 10.** Experimental temperature profiles (red dots) plotted against temperature profiles from CFD analysis (black solid line). The figures show data recorded at 3<sup>rd</sup> and 4<sup>th</sup> window.

Along with the assessment of the new burner performances, insights and data from the experimental campaign were also used as an invaluable tool to verify the reliability of the numerical predictions and, as such, to validate the CFD model as a design tool. On Figure 10, the experimental temperature profiles from in-flame measurement (red dots) are compared against profiles from CFD analysis (black solid line). Despite the complexity of such measure (the in-flame measure is subject to normal oscillations due to the turbulent flows, the length of the probe, the volume of the chamber and few more perturbations) and the complexity of the model, differences between numerical and experimental data remain within a 10% of average deviation, confirming the robustness of the numerical predictions. Similar insights can be obtained when comparing numerical predictions with experimental data collected at the cc exit. On

Figure 11, experimental values from analyzers (red bars) are plotted against values from CFD analysis (blue bars). More particularly, the experimental value of the power produced is obtained from steam data.

As figures clearly show, an excellent match between measured and predicted data is observed. Particularly significant is the NO<sub>x</sub> predictions which is only less than the 3% lower than the experimental value. This suggests, once again, how a detailed numerical model, when supported by an accurate fuel characterization data, could represent a powerful design tool.



**Figure 11.** Experimental values (red bars) plotted against values from CFD analysis (blue bars).

## Conclusions

The design process of a three-flux low-NO<sub>x</sub> 35MW clean coal burner is here presented. The process started with the definition of the design principles to be followed along with the coal and flame pattern to be achieved. Once pinpointed the first geometries to be tested, the design and performance optimization relied entirely on numerical studies. An excellent agreement between numerically predicted and measured data was observed.

This new approach allowed AC-boilers to route its products development to highly efficient burners for power generation purposes while adopting a significantly reduced time to market.

The geometry and performance of the BE4G-35 burner have been further improved afterwards the experimental tests, keeping the new design approach as the starting points for the generation of innovative products. Following this approach, AC-boilers has defined an entire range of coal Multi-Fuel (MF) burners (ranging from 35MW to 65MW) capable of being fuelled in full-firing mode with coal, gas, oil and biomass. The BE4G-45\_MF burner will be tested with coal, natural gas and pellet during the November 2019 experimental test campaign.

In addition, one of the burners of the BE4G range (size to be decided) will be tested in the near future fuelled with low-rank coal to assess the excellent flame stability observed during recent experimental campaign.

## Acknowledgement

The BE4GreenS project has been made possible thanks to the support of *Regione Puglia*.

The authors and AC-BOILERS are grateful to the entire CCA staff for the prototypes manufacturing, assembly and the test-rig set-up.

The authors and AC-BOILERS are grateful to Prof. Victor Scherer and Mr Christian Ontyd from *Ruhr-Universität (LEAT)* for the DTR characterization.

## References

- [1] World energy outlook report, Tech. rep., International Energy Agency (2015).
- [2] Climate change 2014, Tech. rep., Intergovernmental Panel on Climate Change (2014).
- [3] G. D. Rago, G. Rossiello, R. Dadduzio, T. Giani, A. Saponaro, F. Cesareo, M. Lacerenza, F. Fornarelli, G. Caramia, B. Fortunato, S. M. Camporeale, M. Torresi, V. Panebianco, Cfd

- analysis of a swirl stabilized coal combustion burner, *Energy Procedia* 148 (2018) 703–711, aTI 2018 - 73rd Conference of the Italian Thermal Machines Engineering Association.
- [4] M. Torresi, F. Fornarelli, B. Fortunato, S. Camporeale, A. Saponaro, Assessment against experiments of devolatilization and char burnout models for the simulation of an aerodynamically staged swirled low-NO<sub>x</sub> pulverized coal burner, *Energies* 10 (2017) 66.
  - [5] V. V. Ranade, D. F. Gupta, *Computational Modeling of Pulverized Coal Fired Boiler*, 1st Edition, CRC Press, 2015.
  - [6] T. H. Fletcher, A. R. Kerstein, R. J. Pugmire, M. S. Solum, D. M. Grant, Chemical percolation model for devolatilization. direct use of <sup>13</sup>C NMR data to predict effects of coal type, *Energy and Fuels* 6 (4) (1992) 414–431.
  - [7] N. Schaffel, M. Mancini, A. K. Szle, R. Weber, Mathematical modelling of mild combustion of pulverized coal, *Combustion and Flame* 156 (9) (2009) 1771–1784.
  - [8] R. K. Hanson, S. Salimian, *Survey of Rate Constants in the N/H/O System*, Springer New York, New York, NY, 1984, pp. 361–421.
  - [9] G. G. D. Soete, Overall reaction rates of NO and N<sub>2</sub> formation from fuel nitrogen, *Symposium (International) on Combustion* 15 (1) (1975) 1093–1102, fifteenth Symposium (International) on Combustion.
  - [10] M. S. Solum, R. J. Pugmire, D. M. Grant, <sup>13</sup>C solid-state NMR of Argonne premium coals, *Energy and Fuels* 3 (1989) 187–196.
  - [11] M. S. Solum, A. F. Sarofim, R. J. Pugmire, T. H. Fletcher, H. Zhang, <sup>13</sup>C NMR analysis of soot produced from model compounds and coal, *Energy and Fuels* 15 (2001) 961–971.
  - [12] O. M. Moroeng, N. J. Wagner, D. J. Brand, R. J. Roberts, A nuclear magnetic resonance study: Implications for coal formation in the Witbank coalfield, South Africa, *International Journal of Coal Geology* 188 (2018) 45–155.
  - [13] R. C. Uwaoma, C. A. Strydom, R. H. Matjie, J. R. Bunt, G. N. Okolo, D. J. Brand, Pyrolysis of tetralin liquefaction derived residues from lighter density fractions of waste coals taken from waste coal disposal sites in South Africa, *Energy and Fuels* 33 (9) (2019) 9074–9086.
  - [14] S. Heuer, O. Senneca, A. Wutscher, H. Dudder, M. Schiemann, M. Muhler, V. Scherer, Effects of oxy-fuel conditions on the products of pyrolysis in a drop tube reactor, *Fuel Processing Technology* 150 (2016) 41–49.
  - [15] O. Senneca, N. Vorobiev, A. Wuetscher, F. Cerciello, S. Heuer, C. Wedler, R. Span, M. Schiemann, M. Muhler, V. Scherer, Assessment of combustion rates of coal chars for oxy-combustion applications, *Fuel* 238 (2019) 173–185.